Journal of Solid Mechanics Vol. 10, No. 3 (2018) pp. 655-671

Elastic Wave Propagation at Imperfect Boundary of Micropolar Elastic Solid and Fluid Saturated Porous Solid Half-Space

V. Kaliraman [1,*], R.K. Poonia [2]

[1]*Department of Mathematics, Chaudhary Devi Lal University, Sirsa, Haryana, India*
[2]*Department of Mathematics, Chandigarh University, Gharuan, Mohali, Punjab, India*

Received 28 June 2018; accepted 29 August 2018

ABSTRACT

This paper deals with the reflection and transmission of elastic waves from imperfect interface separating a micropolar elastic solid half-space and a fluid saturated porous solid half-space. Longitudinal and transverse waves impinge obliquely at the interface. Amplitude ratios of various reflected and transmitted waves are obtained and computed numerically for a specific model and results obtained are depicted graphically with angle of incidence of incident waves. It is found that these amplitude ratios depend on angle of incidence of the incident wave, imperfect boundary and material properties of half-spaces. From the present study, a special case when fluid saturated porous half-space reduces to empty porous solid is also deduced and discussed graphically.

Keywords : Porous solid; Micro polar elastic solid; Reflection; Transmission; Longitudinal wave; Transverse wave; Amplitude ratios; Stiffness.

1 INTRODUCTION

MOST of natural and man-made materials, including engineering, geological and biological media, possess a microstructure. The ordinary classical theory of elasticity fails to describe the microstructure of the material. To overcome this problem, Eringen and Suhubi [10] considered the microstructure of the material and they showed that the motion in a granular structure material is characterized not by a displacement vector but also by a rotation vector. Gautheir [12] found aluminum-epoxy composite to be a micro polar material. Many problems of waves and vibrations have been discussed in micro polar elastic solid by several researchers. Some of them are Parfitt and Eringen [23], Tomar and Gogna [26], Tomar and Kumar [27], Singh and Kumar [24], Kumar and Barak [18] etc.
On the other side, Brown [4] and de Boer and Ehlers [7-8] developed an interesting theory for porous medium having all constituents to be incompressible. Based on this theory, many researchers like de Boer and Liu [5], Liu [21], de Boer and Didwania [6], Tajuddin and Hussaini [25], Kumar and Hundal [16], Kumari [19], Madan *et al*. [22], Kumar *et al*. [14-15] etc. studied some problems of wave propagation in fluid saturated incompressible porous media. Elastic waves propagation in fluid saturated porous media has its importance in various fields such as soil dynamics, hydrology, seismology, earthquake engineering and geophysics. Imperfect interface considered in this problem means that the stress components are continuous and small displacement field is not. The values of the interface parameters depend upon the material properties of the medium. Recently, using the imperfect conditions at

*Corresponding author. Tel.: +91 94664 04929.
E-mail address: vsisaiya@gmail.com (V. Kaliraman).

the interface, Kumar and Chawla [17], Kumari [20], Kaliraman [13], Barak and Kaliraman [1-2-3] etc. studied the various types of wave problems.

Using the theory of de Boer and Ehlers [8] for fluid saturated porous medium and Eringen [11] for micro polar elastic solid, the reflection and transmission phenomenon of longitudinal and transverse waves at an imperfect interface between micro polar elastic solid half-space and fluid saturated porous solid half-space is studied. A special case when fluid saturated porous solid half-space reduces to empty porous solid half-space has been deduced and discussed. Amplitudes ratios for various reflected and transmitted waves are computed for a particular model and depicted with help of graphs and discussed accordingly. The model which is considered here is assumed to exist in the oceanic crust part of the Earth and the propagation of wave through such a model will be of great use in the fields which are related to Earth sciences.

2 FORMULATION OF THE PROBLEM

Consider a two-dimensional problem by taking the z-axis pointing into the lower half-space and the plane interface $z=0$ separating the fluid saturated porous solid half-space $M_1[z>0]$ and micropolar elastic solid half-space $M_2[z<0]$. A longitudinal wave or transverse wave propagates through the medium M_1 and incident at the plane $z=0$ and making an angle θ_0 with normal to the surface. Corresponding to incident longitudinal or transverse wave, we get two reflected waves in the medium M_1 and three transmitted waves in medium M_2. See Fig. 1.

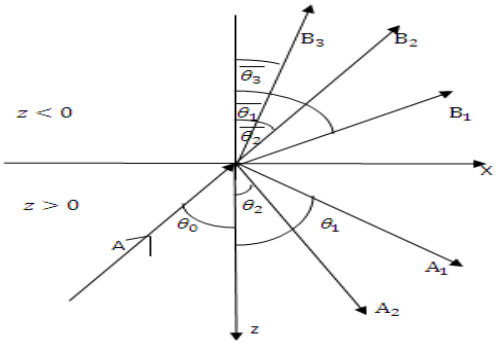

Fig.1
Geometry of the problem.

3 BASIC EQUATIONS AND CONSTITUTIVE RELATIONS

3.1 For medium M_2 (Micro polar elastic solid)

The equation of motion in micro polar elastic medium are given by Eringen [11] as:

$$\left(c_1^2+c_3^2\right)\nabla^2\phi=\frac{\partial^2\phi}{\partial t^2} \tag{1}$$

$$\left(c_2^2+c_3^2\right)\nabla^2\vec{U}+c_3^2\nabla\times\vec{\Phi}=\frac{\partial^2\vec{U}}{\partial t^2} \tag{2}$$

$$\left(c_4^2\nabla^2-2\omega_0^2\right)\vec{\Phi}+\omega_0^2\nabla\times\vec{U}=\frac{\partial^2\vec{\Phi}}{\partial t^2} \tag{3}$$

where

$$c_1^2=\frac{\lambda+2\mu}{\rho};c_2^2=\frac{\mu}{\rho};c_3^2=\frac{\kappa}{\rho};c_4^2=\frac{\gamma}{\rho j};\omega_0^2=\frac{\kappa}{\rho j} \tag{4}$$

Parfitt and Eringen [23] have shown that Eq. (1) corresponds to longitudinal wave propagating with velocity $\overline{v}_1$, given by $\overline{v}_1^2=c_1^2+c_3^2$ and Eqs. (2)-(3) are coupled equations in vector potential $\vec{U}$ and $\vec{\Phi}$ and these correspond to coupled transverse and micro-rotation waves. If $\frac{\omega^2}{\omega_0^2}>2$, there exist two sets of coupled-wave propagating with velocities $\frac{1}{\lambda_2}$ and $\frac{1}{\lambda_3}$; where

$$\lambda_2^2=\frac{1}{2}\left[B-\sqrt{B^2-4C}\right],\lambda_3^2=\frac{1}{2}\left[B+\sqrt{B^2-4C}\right] \tag{5}$$

where,

$$B=\frac{q(p-2)}{\omega^2}+\frac{1}{\left(c_2^2+c_3^2\right)}+\frac{1}{c_4^2};C=\left(\frac{1}{c_4^2}-\frac{2q}{\omega^2}\right)\frac{1}{\left(c_2^2+c_3^2\right)};p=\frac{\kappa}{\mu+\kappa};q=\frac{\kappa}{\gamma} \tag{6}$$

Considering a two-dimensional problem by taking the following components of displacement and micro-rotation as:

$$\vec{u}=(u,0,w)\ \text{ and }\ \vec{\Phi}=(0,\Phi_2,0) \tag{7}$$

where,

$$u=\frac{\partial\phi}{\partial x}-\frac{\partial\psi}{\partial z};\ w=\frac{\partial\phi}{\partial z}+\frac{\partial\psi}{\partial x} \tag{8}$$

and components of stresses are as under

$$t_{zz}=(\psi+2\mu+\kappa)\frac{\partial^2\phi}{\partial z^2}+\lambda\frac{\partial^2\phi}{\partial x^2}+(2\mu+\kappa)\frac{\partial^2\psi}{\partial x\,\partial z} \tag{9}$$

$$t_{zx}=(2\mu+\kappa)\frac{\partial^2\phi}{\partial x\,\partial z}-(\mu+\kappa)\frac{\partial^2\psi}{\partial z^2}+\mu\frac{\partial^2\psi}{\partial x^2}-\kappa\Phi_2 \tag{10}$$

$$m_{zy}=\gamma\frac{\partial\Phi_2}{\partial z} \tag{11}$$

3.2 For medium M_1 (Fluid saturated incompressible porous solid half-space)

Following de Boer and Ehlers [8], the governing equations in a fluid-saturated incompressible porous medium are

$$\operatorname{div}\left(\eta^S\dot{x}_S+\eta^F x_F\right)=0 \tag{12}$$

$$\operatorname{div}T_E^S-\eta^S\operatorname{grad}p+\rho^S\left(b-\ddot{x}_S\right)-P_E^F=0 \tag{13}$$

$$\mathrm{div} T_E^F - \eta^F \mathrm{grad}\, p + \rho^F \left(b - \ddot{x}_F\right) + P_E^F = 0 \tag{14}$$

where $\dot{x}_i$ and $\ddot{x}_i (i = S, F)$ denote the velocities and accelerations, respectively of solid (S) and fluid (F) phases of the porous aggregate and p is the effective pore pressure of the incompressible pore fluid. ρ^S and ρ^F are the densities of the solid and fluid phases respectively and b is the body force per unit volume. T_E^S and T_E^F are the effective stress in the solid and fluid phase respectively. P_E^F is the effective quantity of momentum supply and η^S and η^F are the volume fractions satisfying

$$\eta^S + \eta^F = 1 \tag{15}$$

If u_S and u_F are the displacement vectors for solid and fluid phases, then

$$\dot{x}_S = \dot{u}_S \; ; \; \ddot{x}_S = \ddot{u}_S \; ; \; \dot{x}_F = \dot{u}_F \; ; \; \ddot{x}_F = \ddot{u}_F \tag{16}$$

The constitutive equations for linear isotropic, elastic incompressible porous medium are given by de Boer, Ehlers and Liu [9] as:

$$T_E^S = 2\mu^S E_S + \lambda^S \left(E_S I\right) I \tag{17}$$

$$T_E^F = 0 \tag{18}$$

$$T_E^F = -S_v \left(\dot{u}_F - \dot{u}_S\right) \tag{19}$$

where λ^S and μ^S are the macroscopic Lame's parameters of the porous solid and E_S is the linearized Lagrangian strain tensor defined as:

$$E_S = \frac{1}{2}\left(\mathrm{grad}\, u_S + \mathrm{grad}^T u_S\right) \tag{20}$$

In the case of isotropic permeability, the tensor S_v describing the coupled interaction between the solid and fluid is given by de Boer and Ehlers [8] as:

$$S_v = \frac{\left(\eta^F\right)^2 \gamma^{FR}}{K^F} I \tag{21}$$

where γ^{FR} is the specific weight of the fluid and K^F is the Darcy's permeability coefficient of the porous medium. Making the use of (16) in Eqs. (12)-(14), and with the help of (17)-(20), we obtain

$$\mathrm{div}\left(\eta^S \dot{u}_S + \eta^F \dot{u}_F\right) = 0 \tag{22}$$

$$\left(\lambda^S + \mu^S\right) \mathrm{grad}\, \mathrm{div}\, u_S + \mu^S \mathrm{div}\, \mathrm{grad}\, u_S - \eta^S \mathrm{grad}\, p + \rho^S \left(b - \ddot{u}_S\right) + S_v \left(\dot{u}_F - \dot{u}_S\right) = 0 \tag{23}$$

$$-\eta_F \mathrm{grad}\, p + \rho^F \left(b - \ddot{u}_F\right) - S_v \left(\dot{u}_F - \dot{u}_S\right) = 0 \tag{24}$$

For the two dimensional problem, we assume the displacement vector $u_i \; (i = F, S)$ as:

$$u_i = \left(u^i, 0, w^i\right) \text{ where } i = F, S \tag{25}$$

Eqs. (22) -(24) with the help of Eq. (25) in absence of body forces take the form

$$\eta^S \left[\frac{\partial^2 u^S}{\partial x\,\partial t} + \frac{\partial^2 w^S}{\partial z\,\partial t}\right] + \eta^F \left[\frac{\partial^2 u^F}{\partial x\,\partial t} + \frac{\partial^2 w^F}{\partial z\,\partial t}\right] = 0 \tag{26}$$

$$\eta^F \frac{\partial p}{\partial x} + \rho^F \frac{\partial^2 u^F}{\partial t^2} + S_v \left[\frac{\partial u^F}{dt} - \frac{\partial u^S}{\partial t}\right] = 0 \tag{27}$$

$$\eta^F \frac{\partial p}{\partial z} + \rho^F \frac{\partial^2 w^F}{\partial t^2} + S_v \left[\frac{\partial w^F}{\partial t} - \frac{\partial w^S}{\partial t}\right] = 0 \tag{28}$$

$$\left(\lambda^S + \mu^S\right)\frac{\partial \theta^S}{\partial x} + \mu^S \nabla^2 u^S - \eta^S \frac{\partial p}{\partial x} - \rho^S \frac{\partial^2 u^S}{\partial t^2} + S_v \left[\frac{\partial u^F}{\partial t} - \frac{\partial u^S}{\partial t}\right] = 0 \tag{29}$$

$$\left(\lambda^S + \mu^S\right)\frac{\partial \theta^S}{\partial z} + \mu^S \nabla^2 w^S - \eta^S \frac{\partial p}{\partial z} - \rho^S \frac{\partial^2 w^S}{\partial t^2} + S_v \left[\frac{\partial w^F}{\partial t} - \frac{\partial w^S}{\partial t}\right] = 0 \tag{30}$$

where,

$$\theta^S = \frac{\partial\left(u^S\right)}{\partial x} + \frac{\partial\left(w^S\right)}{\partial z} \tag{31}$$

and

$$\nabla^2 = \frac{\partial^2}{\partial x^2} + \frac{\partial^2}{\partial z^2} \tag{32}$$

Also, t_{zz}^S and t_{zx}^S the normal and tangential stresses in the solid phase are as under

$$t_{zz}^S = \lambda^S \left(\frac{\partial u^S}{\partial x} + \frac{\partial w^S}{\partial z}\right) + 2\mu^S \frac{\partial w^S}{\partial z} \tag{33}$$

$$t_{zx}^S = \mu^S \left(\frac{\partial u^S}{\partial z} + \frac{\partial w^S}{\partial x}\right) \tag{34}$$

The displacement components u^j and w^j are related to the dimensional potential ϕ^j and ψ^j as:

$$u^j = \frac{\partial \phi^j}{\partial x} + \frac{\partial \psi^j}{\partial z}\ ;\ w^j = \frac{\partial \phi^j}{\partial z} - \frac{\partial \psi^j}{\partial x}\ ;\ j = S, F \tag{35}$$

Using Eq. (35) in Eqs. (26)-(30), we obtain the following equations determining ϕ^S , ϕ^F , ψ^S , ψ^F and p as:

$$\nabla^2\phi^S - \frac{1}{C_1^2}\frac{\partial^2\phi^S}{\partial t^2} - \frac{S_v}{\left(\lambda^S + 2\mu^S\right)\left(\eta^F\right)^2}\frac{\partial\phi^S}{\partial t} = 0 \tag{36}$$

$$\phi^F = -\frac{\eta^S}{\eta^F}\phi^S \tag{37}$$

$$\mu^S\nabla^2\psi^S - \rho^S\frac{\partial^2\psi^S}{\partial t^2} + S_v\left[\frac{\partial\psi^F}{\partial t} - \frac{\partial\psi^S}{\partial t}\right] = 0 \tag{38}$$

$$\rho^F\frac{\partial^2\psi^F}{\partial t^2} + S_v\left[\frac{\partial\psi^F}{\partial t} - \frac{\partial\psi^S}{\partial t}\right] = 0 \tag{39}$$

$$\left(\eta^F\right)^2 p - \eta^S\rho^F\frac{\partial^2\phi^S}{\partial t^2} - S_v\frac{\partial\phi^S}{\partial t} = 0 \tag{40}$$

where,

$$C_1 = \sqrt{\frac{\left(\eta^F\right)^2\left(\lambda^S + 2\mu^S\right)}{\left(\eta^F\right)^2\rho^S + \left(\eta^S\right)^2\rho^F}} \tag{41}$$

Assuming the solution of the system of Eqs. (36) -(40) in the form

$$\left(\phi^S, \phi^F, \psi^S, \psi^F, p\right) = \left(\phi_1^S, \phi_1^F, \psi_1^S, \psi_1^F, p_1\right)\exp\left(i\omega t\right) \tag{42}$$

where ω is the complex circular frequency.

Making the use of Eq. (42) in Eqs. (36) -(40), we obtain

$$\left[\nabla^2 + \frac{\omega^2}{C_1^2} - \frac{i\omega S_v}{\left(\lambda^S + 2\mu^S\right)\left(\eta^F\right)^2}\right]\phi_1^S = 0 \tag{43}$$

$$\left[\mu^S\nabla^2 + \rho^S\omega^2 - i\omega S_v\right]\psi_1^S = -i\omega S_v\psi_1^F \tag{44}$$

$$\left[-\omega^2\rho^F + i\omega S_v\right]\psi_1^{\$} - i\omega S_v\psi_1^S = 0 \tag{45}$$

$$\left(\eta^F\right)^2 p_1 + \eta^S\rho^F\omega^2\phi_1^S - i\omega S_v\phi_1^S = 0 \tag{46}$$

$$\phi_1^F = -\frac{\eta^S}{\eta^F}\phi_1^S \tag{47}$$

Eq. (43) corresponds to longitudinal wave propagating with velocity v_1, given by

$$v_1^2 = \frac{1}{G_1} \tag{48}$$

where,

$$G_1 = \left[\frac{1}{C_1^2} - \frac{iS_v}{\omega\left(\lambda^S + 2\mu^S\right)\left(\eta^F\right)^2} \right] \tag{49}$$

From Eqs. (44) and (45), we obtain

$$\left[\nabla^2 + \frac{\omega^2}{v_2^2} \right] \psi_1^S = 0 \tag{50}$$

Eq. (50) corresponds to transverse wave propagating with velocity v_2, given by $v_2^2 = \frac{1}{G_2}$, where

$$G_2 = \left\{ \frac{\rho^S}{\mu^S} - \frac{iS_v}{\mu^S \omega} - \frac{S_v^2}{\mu^S\left(-\rho^S \omega^2 + i\,\omega S_v\right)} \right\} \tag{51}$$

4 SOLUTION OF THE GOVERNING EQUATIONS

For medium M_2, let us consider

$$\phi = B_1 \exp\left[i\,\delta_1 \left(x \sin\bar{\theta}_1 - z \cos\bar{\theta}_1 \right) + i\,\bar{\omega}_1 t \right] \tag{52}$$

$$\psi = B_2 \exp\left\{ i\,\delta_2 \left(x \sin\bar{\theta}_2 - z \cos\bar{\theta}_2 \right) + i\,\bar{\omega}_2 t \right\} + B_3 \exp\left\{ i\,\delta_3 \left(x \sin\bar{\theta}_3 - z \cos\bar{\theta}_3 \right) + i\,\bar{\omega}_3 t \right\} \tag{53}$$

$$\Phi_2 = EB_2 \exp\left\{ i\,\delta_2 \left(x \sin\bar{\theta}_2 - z \cos\bar{\theta}_2 \right) + i\,\bar{\omega}_2 t \right\} + FB_3 \exp\left\{ i\,\delta_3 \left(x \sin\bar{\theta}_3 - z \cos\bar{\theta}_3 \right) + i\,\bar{\omega}_3 t \right\}, \tag{54}$$

where

$$E = \frac{\delta_2^2 \left(\delta_2^2 - \dfrac{\omega^2}{\left(c_2^2 + c_3^2\right)} + pq \right)}{\text{deno.}} \tag{55}$$

$$F = \frac{\delta_3^2 \left(\delta_3^2 - \dfrac{\omega^2}{\left(c_2^2 + c_3^2\right)} + pq \right)}{\text{deno.}} \tag{56}$$

and

$$deno = p\left(2q - \frac{\omega^2}{c_4^2} \right);\ \delta_2^2 = \lambda_2^2 \omega^2;\ \delta_3^2 = \lambda_3^2 \omega^2 \tag{57}$$

and for medium M_1, we take

$$\left\{ \phi^S, \phi^F, p \right\} = \left\{ 1, m_1, m_2 \right\} \left[A_{01} \exp\left\{ ik_1 \left(x \sin\theta_0 - z \cos\theta_0 \right) + i\,\omega_1 t \right\} + A_1 \exp\left\{ ik_1 \left(x \sin\theta_1 + z \cos\theta_1 \right) + i\,\omega_1 t \right\} \right] \tag{58}$$

$$\left\{\psi^S,\psi^F\right\}=\left\{1,m_3\right\}\left[B_{01}\exp\left\{ik_2\left(x\,\sin\theta_0-z\,\cos\theta_0\right)+i\,\omega_2 t\right\}+A_2\exp\left\{ik_2\left(x\,\sin\theta_2+z\,\cos\theta_2\right)+i\,\omega_2 t\right\}\right] \tag{59}$$

where,

$$m_1=-\frac{\eta^S}{\eta^F}\;;\; m_2=-\left[\frac{\eta^S\omega_1^2\rho^F-i\,\omega_1 S_v}{\left(\eta^F\right)^2}\right]\;;\; m_3=\frac{i\,\omega_2 S_V}{i\,\omega\,S_V-\omega_2^2\rho^F} \tag{60}$$

and B_1, B_2, B_3 are amplitudes of transmitted *P*-wave, transmitted coupled transverse and transmitted micro-rotation waves respectively. Also A_{01} or B_{01}, A_1 and A_2 are amplitudes of incident *P*-wave or SV-wave, reflected *P*-wave and reflected SV-wave respectively and to be determined from boundary conditions.

5 BOUNDARY CONDITIONS

Boundary conditions appropriate here are the continuity of displacement, micro rotation and stresses at the interface separating medium M_1 and M_2. These boundary conditions at $z = 0$ can be written in mathematical form as:

$$t_{zz}=t_{zz}^S-p\;;\; t_{zx}=t_{zx}^S\;;\; m_{zy}=0\;;\; t_{zz}^S-p=K_n\left(w-w^S\right);\; t_{zx}^S=K_t\left(u-u^S\right) \tag{61}$$

where K_n and K_t are normal and tangential stiffness coefficient.

In order to satisfy the boundary conditions, the extension of the Snell's law will be

$$\frac{\sin\theta_0}{v_0}=\frac{\sin\theta_1}{v_1}=\frac{\sin\theta_2}{v_2}=\frac{\sin\bar{\theta}_1}{\bar{v}_1}=\frac{\sin\bar{\theta}_2}{\bar{v}_2}=\frac{\sin\bar{\theta}_3}{\bar{v}_3} \tag{62}$$

where, $\bar{v}_2=\dfrac{1}{\lambda_z}$; $\bar{v}_3=\dfrac{1}{\lambda_3}$. For longitudinal wave,

$$v_0=v_1,\;\theta_0=\theta_1 \tag{63}$$

For transverse wave,

$$v_0=v_2,\;\theta_0=\theta_2 \tag{64}$$

Also

$$\delta_1\bar{v}_1=\delta_2\lambda_2^{-1}=\delta_3\lambda_3^{-1}=k_1v_1=k_2v_2=\omega\;,\quad z=0 \tag{65}$$

Making the use of potentials given by Eqs . (52)-(54) and (58)-(59) in the boundary conditions given by Eq. (61) and using (62)-(65), we get a system of five non-homogeneous equations which can be written as:

$$\sum_{j=1}^{5}a_{ij}Z_j=Y_i\,,\quad\left(i=1,2,3,4,5\right) \tag{66}$$

where

$$Z_1=\frac{B_1}{B_0}\ ;\ Z_2=\frac{B_2}{B_0}\ ;\ Z_3=\frac{B_3}{B_0}\ ;\ Z_4=\frac{A_1}{B_0}\ ;\ Z_5=\frac{A_2}{B_0} \tag{67}$$

where $B_0=A_{01}$ or B_{01} is amplitude of incident *P*-wave or SV-wave respectively.

Also Z_1 to Z_5 are the amplitude ratios of transmitted longitudinal wave, transmitted coupled-wave at an angle $\bar{\theta}_2$, transmitted coupled-wave at an angle $\bar{\theta}_3$, reflected *P*-wave and reflected SV-wave, respectively. Also a_{ij} and Y_i in non-dimensional form are as:

$$a_{11}=\frac{-\lambda\delta_1^2-(2\mu+\kappa)\left(\delta_1^2\cos^2\bar{\theta}_1\right)}{\mu\delta_1^2}\ ;\ a_{12}=\frac{(2\mu+\kappa)\delta_2^2\sin\bar{\theta}_2\cos\bar{\theta}_2}{\mu\delta_1^2}\ ;\ a_{13}=\frac{(2\mu+\kappa)\delta_3^2\sin\bar{\theta}_3\cos\bar{\theta}_3}{\mu\delta_1^2}\ ;$$

$$a_{14}=\frac{k_1^2\left(\lambda^S+2\mu^S\cos^2\theta_1\right)+m_2}{\mu\delta_1^2}\ ;\ a_{15}=\frac{-2\mu^S k_2^2\sin\theta_2\cos\theta_2}{\mu\delta_1^2}\ ;\ a_{21}=\frac{(2\mu+\kappa)\delta_1^2\sin\bar{\theta}_3\cos\bar{\theta}_1}{\mu\delta_1^2}\ ;$$

$$a_{22}=\frac{\mu\delta_2^2\cos2\bar{\theta}_2+\kappa\delta_2^2\cos^2\bar{\theta}_2-\kappa E}{\mu\delta_1^2}\ ;\ a_{23}=\frac{\mu\delta_3^2\cos2\bar{\theta}_3+\kappa\delta_3^2\cos^2\bar{\theta}_3-\kappa F}{\mu\delta_1^2}\ ;\ a_{24}=\frac{\mu^S k_1^2\sin2\theta_1}{\mu\delta_1^2}\ ;$$

$$a_{25}=\frac{\mu^S k_2^2\cos2\theta_2}{\mu\delta_1^2}\ ;\ a_{31}=0\ ;\ a_{32}=\cos\bar{\theta}_2\ ;\ a_{33}=\frac{\delta_3 F\cos\bar{\theta}_3}{\delta_2 E}\ ;\ a_{34}=0\ ;\ a_{35}=0\ ;$$

$$a_{41}=\frac{\lambda\delta_1^2+(2\mu+\kappa)\left(\delta_1^2\cos^2\bar{\theta}_1\right)+k_n i\,\delta_1\cos\bar{\theta}_1}{k_n\delta_1}\ ;\ a_{42}=\frac{-(2\mu+\kappa)\delta_2^2\sin\bar{\theta}_2\cos\bar{\theta}_2-k_n i\,\delta_2\sin\bar{\theta}_2}{k_n\delta_1}\ ;$$

$$a_{43}=\frac{-(2\mu+\kappa)\delta_3^2\sin\bar{\theta}_3\cos\bar{\theta}_3-k_n i\,\delta_3\sin\bar{\theta}_3}{k_n\delta_1}\ ;\ a_{44}=\frac{ik_1\cos\theta_1}{\delta_1}\ ;\ a_{45}=-\frac{ik_2\sin\theta_2}{\delta_1}$$

$$a_{51}=\frac{-(2\mu+\kappa)\delta_1^2\sin\bar{\theta}_1\cos\bar{\theta}_1-ik_t\delta_1\sin\bar{\theta}_1}{k_t\delta_1}\ ;\ a_{53}=\frac{-\mu\delta_3^2\cos2\bar{\theta}_3-\kappa\delta_3^2\cos^2\bar{\theta}_3+\kappa F-k_t\delta_3\cos\bar{\theta}_3}{k_t\delta_1}\ ;$$

$$a_{54}=\frac{ik_1\sin\theta_1}{\delta_1}\ ;\ a_{55}=\frac{ik_2\cos\theta_2}{\delta_1}$$

For incident *P*-wave

$$Y_1=-a_{14}\ ;\ Y_2=a_{24}\ ;\ Y_3=a_{34}\ ;\ Y_4=a_{44}\ ;\ Y_5=-a_{54}.$$

For incident SV wave

$$Y_1=a_{15}\ ;\ Y_2=-a_{25}\ ;\ Y_3=a_{35}\ ;\ Y_4=-a_{45}\ ;\ Y_5=a_{55} \tag{68}$$

6 PARTICULAR CASE: WELDED CONTACT $\left(K_n\to\infty, K_t\to\infty\right)$

Again in this case, a system of five non-homogeneous equations is obtained as in Eq. (68) with some a_{ij} changed as:

$$a_{41}=\frac{i\,\delta_1\cos\bar{\theta}_1}{\delta_1}\ ;\ a_{42}=\frac{-i\,\delta_2\sin\bar{\theta}_2}{\delta_1}\ ;\ a_{43}=\frac{-i\,\delta_3\sin\bar{\theta}_3}{\delta_1}\ ;\ a_{51}=-i\sin\bar{\theta}_1\ ;\ a_{52}=\frac{-i\,\delta_2\cos\bar{\theta}_2}{\delta_1}\ ;$$
$$a_{53}=\frac{-i\,\delta_3\cos\bar{\theta}_3}{\delta_1} \tag{69}$$

7 SPECIAL CASE

If pores are absent or gas is filled in the pores then ρ^F is very small as compared to ρ^S and can be neglected, so the relation (41) gives us

$$C = \sqrt{\frac{\lambda^S + 2\mu^S}{\rho^S}} \tag{70}$$

In this situation the problem reduces to the problem to empty porous solid half-space lying over micro polar elastic solid half-space.

8 NUMERICAL RESULTS AND DISCUSSION

In order to study in more detail, the behavior of various amplitude ratios, we have computed them numerically for a particular model for which the values of relevant elastic parameters are as follow:

In medium M_1, the physical constants for fluid saturated incompressible porous medium are taken from de Boer, Ehlers and Liu [9] as:

$$\eta^S = 0.67,\ \eta^F = 0.33,\ \rho^S = 1.34\ \text{Mg/m}^3,\ \rho^F = 0.33\ \text{Mg/m}^3,\ \lambda^S = 5.5833\ \text{MN/m}^2,$$
$$K^F = 0.01\ \text{m/s},\ \gamma^{FR} = 10.00\ \text{KN/m}^3,\ \mu^S = 8.3750\ \text{N/m}^2$$

In medium M_2, the physical constants for micro polar elastic solid are taken from Gauthier [12] as:

$$\lambda = 7.59\times10^{10}\ \text{N/m}^2,\ \mu = 1.89\times10^{10}\ \text{N/m}^2,\ \kappa = 1.49\times10^{8}\ \text{N/m}^2,\ \rho = 2.19\times10^{3}\ \text{kg/m}^3,$$
$$\gamma = 2.68\times10^{4}\ \text{N},\ j = 1.96\times10^{-6}\ \text{m}^2,\ \frac{\omega^2}{\omega_0^2} = 200 \tag{71}$$

To calculate the modulus of amplitude ratios of various reflected and transmitted waves for the particular model and to depict graphically, a computer program in MATLAB has been developed. The amplitude ratios are computed for the angle of incidence varying from 0° to 90°. The variation of modulus of amplitude ratios Z_i with angle of emergence θ_0 of longitudinal *P*-wave or transverse SV wave are shown in Figs. (2)-(31). In Figs. (2)-(21) dotted lines show the variations of amplitude ratios $|Z_i|$ when medium-M_1 is incompressible fluid saturated porous medium (FS) and medium-M_{II} is micro polar elastic solid and boundary between half-space is imperfect whereas solid lines show the variations of amplitude ratios when contact between half-spaces is welded. In Figs. (2) -(6), there is *P*-wave incident whereas in Figs. (7) -(11), SV wave is incident. In Figs. (12) -(16), there is *P*-wave incident and incompressible fluid saturated porous medium (FS) becomes empty porous solid (EPS) whereas in Figs. (17)-(21), SV wave is incident and medium-M_1 is empty porous solid. The nature of dependence of modulus of amplitude ratios Z_i on *P*-wave or SV is shown in Figs. (22)-(31). The nature of dependence of modulus of amplitude ratios Z_i is different for different reflected and transmitted waves.

8.1 Longitudinal wave incidence

The Figs. (2)-(6), show the variations of the modulus of amplitude ratios of reflected *P*-wave i.e. $|Z_4|$, reflected SV wave i.e. $|Z_5|$, transmitted *P*-wave i.e. $|Z_1|$, transmitted CDI-wave i.e. $|Z_2|$, and transmitted CDII-wave i.e. $|Z_3|$, with angle of incidence of incident *P*-wave. In Figs. (2) -(6), the effect of welded contact is significant to general stiffness case (imperfect interface) and is clear from the graphs. Also, in Figs. (12) -(16), in case of empty porous solid, the effect of stiffness is clear. In these figures, the modulus value of amplitudes ratios for imperfect interface

is small than all other cases except in Figs. (5) and (15)-(16). The effect of fluid filled in pores of fluid saturated porous medium is evident after comparing the corresponding Figs. (2)-(6) and (12)-(16).

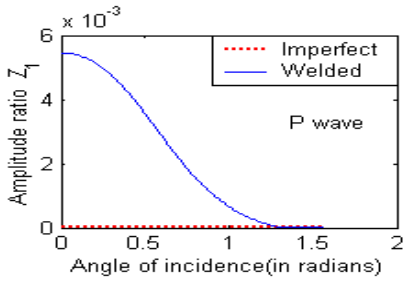

Fig.2
Variation of the amplitude ratio $|Z_i|$, i=1, 2,…,5 with angle of incidence of incident *P*-wave.

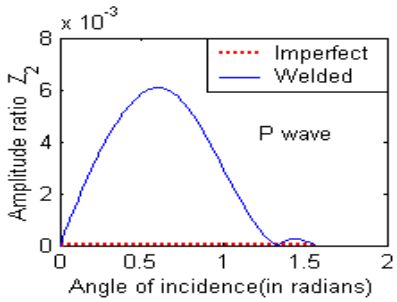

Fig.3
Variation of the amplitude ratio $|Z_i|$, i=1, 2,…,5 with angle of incidence of incident *P*-wave.

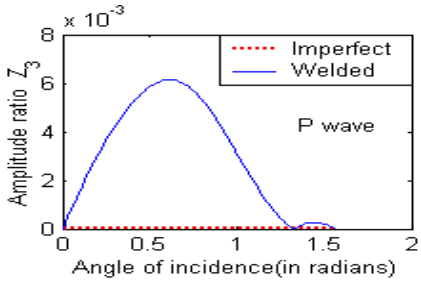

Fig.4
Variation of the amplitude ratio $|Z_i|$, i=1, 2,…,5 with angle of incidence of incident *P*-wave.

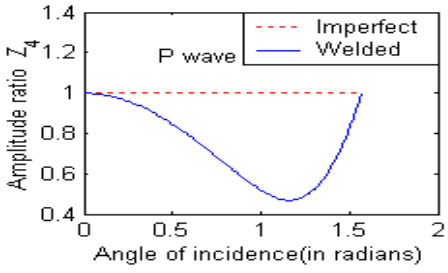

Fig.5
Variation of the amplitude ratio $|Z_i|$, i=1, 2,…,5 with angle of incidence of incident *P*-wave.

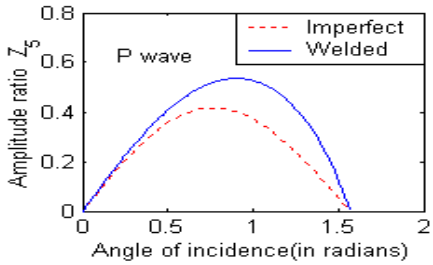

Fig.6
Variation of the amplitude ratio $|Z_i|$, i=1, 2,…,5 with angle of incidence of incident *P*-wave.

8.2 Transverse wave incidence

The Figs. (7) -(11), show the variation of the modulus of amplitude ratios of reflected *P*-wave, reflected SV wave, transmitted *P*-wave, transmitted CDI-wave, and transmitted CDII-wave, with angle of incidence of incident SV-wave. In the Figs. (7) -(11), the amplitude ratios are small for imperfect boundary in comparison to welded contact except in Fig. (11). Also, in Figs. (17) -(21), in case of empty porous solid, the effect of stiffness is clear and amplitude ratios are small for imperfect interface in comparison to welded contact. After comparing the corresponding Figs. (7) -(11) and (17) -(21), the effect of fluid filled in pores of fluid saturated porous medium is clear.

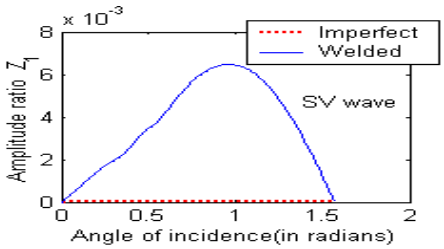

Fig.7
Variation of the amplitude ratio $|Z_i|$, i=1,2,…,5 with angle of incidence of incident SV wave.

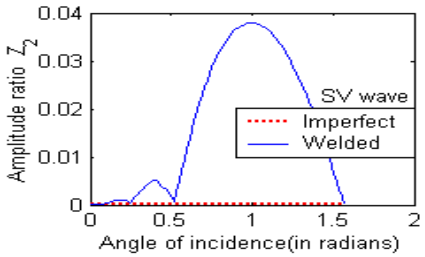

Fig.8
Variation of the amplitude ratio $|Z_i|$, i=1,2,…,5 with angle of incidence of incident SV wave.

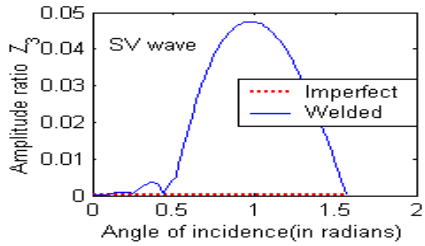

Fig.9
Variation of the amplitude ratio $|Z_i|$, i=1,2,…,5 with angle of incidence of incident SV wave.

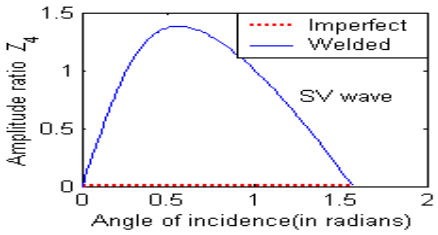

Fig.10
Variation of the amplitude ratio $|Z_i|$, i=1,2,…,5 with angle of incidence of incident SV wave.

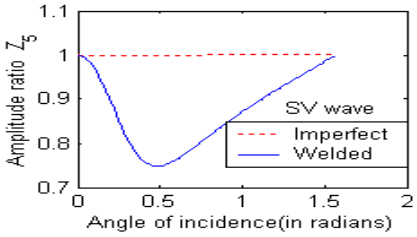

Fig.11
Variation of the amplitude ratio $|Z_i|$, i=1,2,…,5 with angle of incidence of incident SV wave.

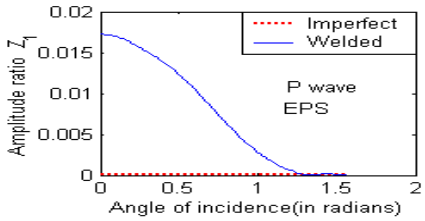

Fig.12
Variation of the amplitude ratio $|Z_i|$ i=1, 2,…,5 with angle of incidence of incident *P*- wave for empty porous solid.

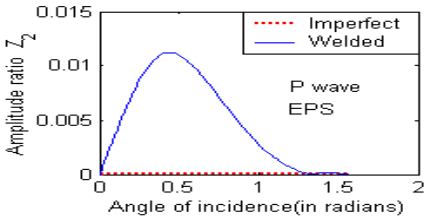

Fig.13
Variation of the amplitude ratio $|Z_i|$ i=1, 2,…,5 with angle of incidence of incident *P*- wave for empty porous solid.

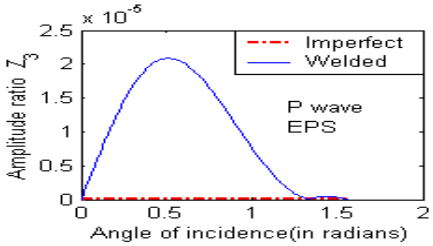

Fig.14
Variation of the amplitude ratio $|Z_i|$ i=1, 2,…,5 with angle of incidence of incident *P*- wave for empty porous solid.

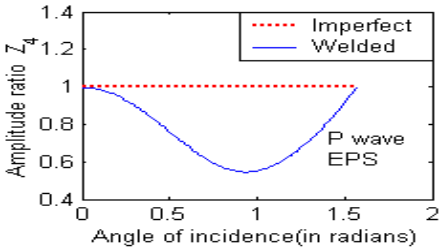

Fig.15
Variation of the amplitude ratio $|Z_i|$ i=1, 2,…,5 with angle of incidence of incident *P*- wave for empty porous solid.

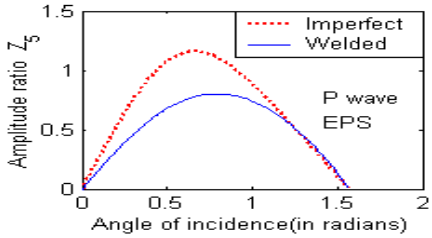

Fig.16
Variation of the amplitude ratio $|Z_i|$ i=1, 2,…,5 with angle of incidence of incident *P*- wave for empty porous solid.

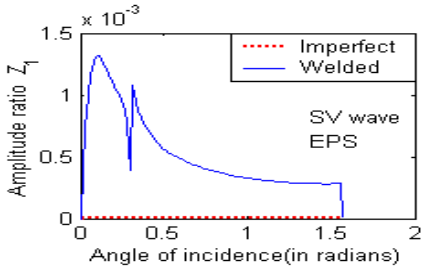

Fig.17
Variation of the amplitude ratio $|Z_i|$ i=1, 2,…,5 with angle of incidence of incident SV wave for empty porous solid.

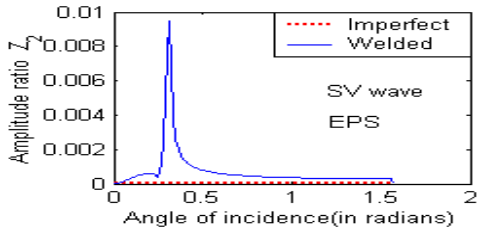

Fig.18
Variation of the amplitude ratio $|Z_i|$ i=1, 2,…,5 with angle of incidence of incident SV wave for empty porous solid.

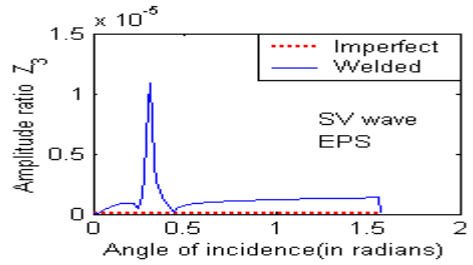

Fig.19
Variation of the amplitude ratio $|Z_i|$ i=1, 2,…,5 with angle of incidence of incident SV wave for empty porous solid.

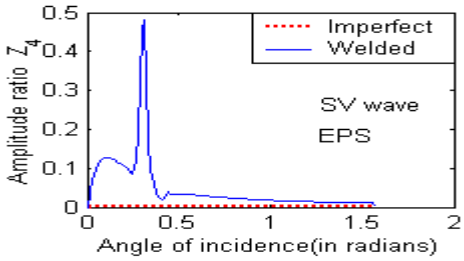

Fig.20
Variation of the amplitude ratio $|Z_i|$ i=1, 2,…,5 with angle of incidence of incident SV wave for empty porous solid.

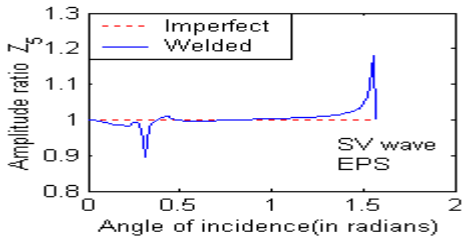

Fig.21
Variation of the amplitude ratio $|Z_i|$ i=1, 2,…,5 with angle of incidence of incident SV wave for empty porous solid.

8.3 P-wave or SV wave incidence

Figs. (22) -(26) depicts the effect of incident longitudinal and incident transverse wave on the variation of amplitude ratios. From these figures it is very clear that the amplitude ratios depend on incident wave. Also, the amplitude ratios are small for incident *P*- wave in comparison to SV wave except for modulus of amplitude ratio of reflected *P*-wave i.e. $|Z_4|$. Effect of incident longitudinal or incident transverse wave on the variation of amplitude ratios in case of empty porous solid is shown in Figs. (27) - (31). In these figures, the modulus of amplitude ratios for transmitted waves, are large in case of SV wave incidence and small for reflected waves.

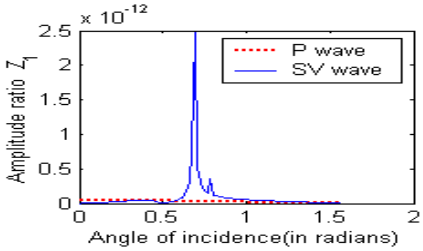

Fig.22
Variation of the amplitude ratio $|Z_i|$, i=1, 2,…,5 with angle of incidence of incident *P*- wave or SV wave.

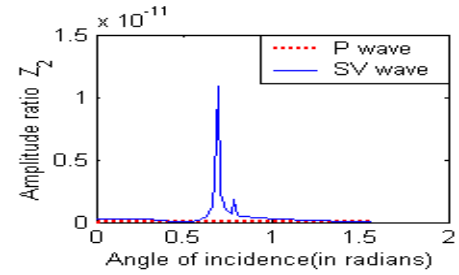

Fig.23
Variation of the amplitude ratio $|Z_i|$, i=1, 2,…,5 with angle of incidence of incident *P*-wave or SV wave.

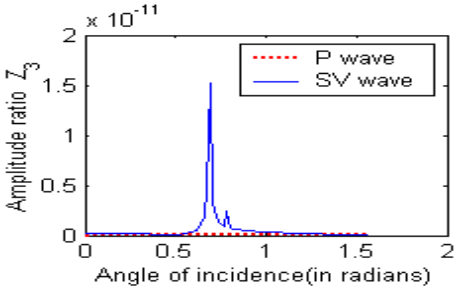

Fig.24
Variation of the amplitude ratio $|Z_i|$, i=1, 2,…,5 with angle of incidence of incident *P*- wave or SV wave.

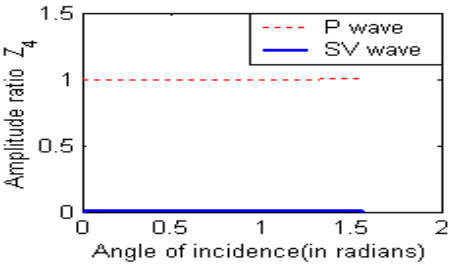

Fig.25
Variation of the amplitude ratio $|Z_i|$, i=1, 2,…,5 with angle of incidence of incident *P*- wave or SV wave.

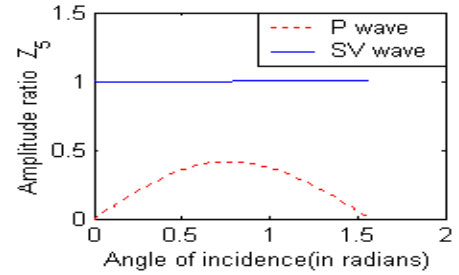

Fig.26
Variation of the amplitude ratio $|Z_i|$, i=1, 2,…,5 with angle of incidence of incident *P*- wave or SV wave.

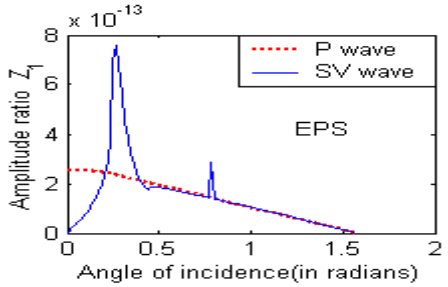

Fig.27
Variation of the amplitude ratio $|Z_i|$ with angle of incidence of incident *P*- wave or SV wave for empty porous solid.

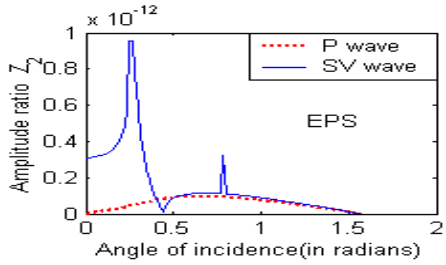

Fig.28
Variation of the amplitude ratio $|Z_i|$ with angle of incidence of incident *P*- wave or SV wave for empty porous solid.

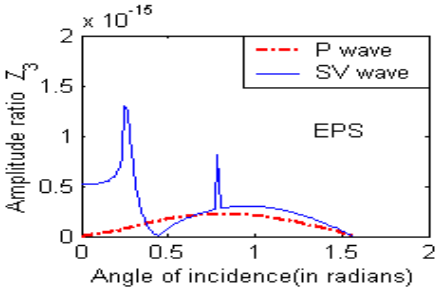

Fig.29
Variation of the amplitude ratio $|Z_i|$ with angle of incidence of incident *P*- wave or SV wave for empty porous solid.

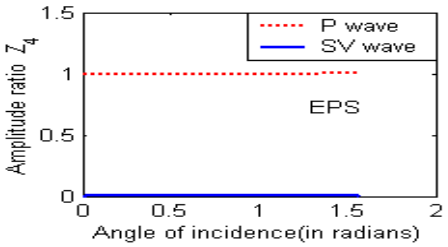

Fig.30
Variation of the amplitude ratio $|Z_i|$ with angle of incidence of incident *P*- wave or SV wave for empty porous solid.

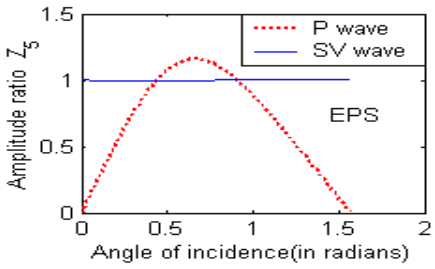

Fig.31
Variation of the amplitude ratio $|Z_i|$ with angle of incidence of incident *P*- wave or SV wave for empty porous solid.

9 CONCLUSIONS

In conclusion, a mathematical study of reflection and transmission coefficient at an imperfect interface separating micro polar elastic solid half-space and fluid saturated incompressible porous solid half space is made when longitudinal wave or transverse wave is incident. It is observed that

1. The amplitudes ratios of various reflected and transmitted waves are found to be complex valued.
2. The modulus of amplitudes ratios of various reflected and transmitted waves depend on the angle of incidence of the incident wave and material properties of half-spaces.
3. The effect of fluid filled in the pores of incompressible fluid saturated porous medium is significant on the amplitudes ratios.
4. The effect of incident wave is significant on amplitude ratios. All the amplitudes ratios are found to depend on incident waves.
5. The effect of stiffness is significant either longitudinal wave is incident or transverse wave is incident.

The model presented in this paper is one of the more realistic forms of the Earth models. The present theoretical results may provide useful information for experimental scientists/researchers/seismologists working in the area of wave propagation in micropolar elastic solid and fluid saturated incompressible porous solid.

REFERENCES

[1] Barak M.S., Kaliraman V., 2017, Reflection and refraction phenomena of elastic wave propagating through imperfect interface of solids, *International Journal of Statistika and Mathematika* **24**(1): 01-11.

[2] Barak M.S., Kaliraman V., 2018, Propagation of elastic waves at micro polar viscoelastic solid/fluid saturated incompressible porous solid interface, *International Journal of Computational Methods* **15**(1): 1850076(1-19).

[3] Barak M.S., Kaliraman V., 2018, Reflection and transmission of elastic waves from an imperfect boundary between micro polar elastic solid half space and fluid saturated porous solid half space, *Mechanics of Advanced Materials and Structures* **2018**: 1-8.

[4] Bowen R.M., 1980, Incompressible porous media models by use of the theory of mixtures, *International Journal of Engineering Science* **18**: 1129-1148.

[5] De Boer R., Liu Z., 1994, Plane waves in a semi-infinite fluid saturated porous medium, *Transport in Porous Media* **16**(2): 147-173.

[6] De Boer R., Didwania A.K., 2004, Two phase flow and capillarity phenomenon in porous solid- A *Continuum Thermomechanical Approach, Transport in Porous Media* **56**: 137-170.

[7] De Boer R., Ehlers W., 1990, The development of the concept of effective stress, *Acta Mechanica* **83**: 77-92.

[8] De Boer R., Ehlers W., 1990, Uplift friction and capillarity-three fundamental effects for liquid-saturated porous solids, *International Journal of Solids and Structures* **26**: 43-47.

[9] De Boer R., Ehlers W., Liu Z., 1993, One-dimensional transient wave propagation in fluid-saturated incompressible porous media, *Archive of Applied Mechanics* **63**(1): 59-72.

[10] Eringen A.C., Suhubi E.S., 1964, Nonlinear theory of simple micro-elastic solids I, *International Journal of Engineering Science* **2**: 189-203.

[11] Eringen A.C., 1968, Linear theory of micro polar elasticity, *International Journal of Engineering Science* **5**: 191-204.

[12] Gautheir R.D., 1982, *Experimental Investigations on Micro polar Media, Mechanics of Micro polar Media*, World Scientific, Singapore.

[13] Kaliraman V., 2016, Propagation of *P* and SV waves through loosely bonded solid/solid interface, *International Journal of Mathematics Trends and Technology* **52**(6): 380-392.

[14] Kumar R., Madan D.K., Sikka J.S., 2014, Shear wave propagation in multilayered medium including an irregular fluid saturated porous stratum with rigid boundary, *Advances in Mathematical Physics* **2014**: 163505.

[15] Kumar R., Madan D.K., Sikka J.S., 2015, Wave propagation in an irregular fluid saturated porous anisotropic layer sandwiched between a homogeneous layer and half space, *Wseas Transactions on Applied and Theoretical Mechanics* **10**: 62-70.

[16] Kumar R., Hundal B.S., 2007, Surface wave propagation in fluid-saturated incompressible porous medium, *Sadhana* **32** (3): 155-166.

[17] Kumar R., Chawla V., 2010, Effect of rotation and stiffness on surface wave propagation in elastic layer lying over a generalized thermo-diffusive elastic half-space with imperfect boundary, *Journal of Solid Mechanics* **2**(1): 28-42.

[18] Kumar R., Barak M., 2007, Wave propagation in liquid-saturated porous solid with micro polar elastic skeleton at boundary surface, *Applied Mathematics and Mechanics* **28**(3): 337-349.

[19] Kumari N., 2014, Reflection and transmission of longitudinal wave at micro polar viscoelastic solid/fluid saturated incompressible porous solid interface, *Journal of Solid Mechanics* **6**(3): 240-254.

[20] Kumari N., 2014, Reflection and transmission phenomenon at an imperfect boundary of viscoelastic solid and fluid saturated incompressible porous solid, *Bulletin of Mathematics and Statistics Research* **2**(3): 306-319.

[21] Liu Z., 1999, Propagation and evolution of wave fronts in two-phase porous media, *Transport in Porous Media* **34**: 209-225.

[22] Madan D.K., Kumar R., Sikka J.S., 2014, Love wave propagation in an irregular fluid saturated porous anisotropic layer with rigid boundary, *Journal of Applied Sciences Research* **10**(4): 281 - 287.

[23] Parfitt V.R., Eringen A.C., 1969, Reflection of plane waves from the flat boundary of a micro polar elastic half-space, *Journal of the Acoustical Society of America* **45**: 1258-1272.

[24] Singh B., Kumar R., 2007, Wave reflection at viscoelastic-micro polar elastic interface, *Applied Mathematics and Computation* **185**: 421-431.

[25] Tajuddin M., Hussaini S.J., 2006, Reflection of plane waves at boundaries of a liquid filled poroelastic half-space, *Journal Applied Geophysics* **58**: 59-86.

[26] Tomar S.K., Gogna M.L., 1992, Reflection and refraction of longitudinal micro rotational wave at an interface between two different micro polar elastic solids in welded contact, *International Journal of Engineering Science* **30**: 1637-1646.

[27] Tomar S.K., Kumar R., 1995, Reflection and refraction of longitudinal displacement wave at a liquid micro polar solid interface, *International Journal Engineering Sciences* **33**: 1507-1515.